

# Witnessing globular cluster formation at $z \sim 3-10$ with JWST and ELT

Alvio Renzini<sup>ID</sup>

INAF – Osservatorio Astronomico di Padova, Vicolo dell’Osservatorio 5, 35122, Padova, Italy  
email: [alvio.renzini@inaf.it](mailto:alvio.renzini@inaf.it)

**Abstract.** The opportunities offered by JWST and the ELT for the detection and study of forming/just formed globular clusters at high redshifts are illustrated, also alluding at the unique insight we may get on the very early stages of galaxy formation.

**Keywords.** globular clusters: general, galaxies: high-redshift, galaxies: evolution, galaxies: formation, galaxies: star clusters.

---

## 1. Introduction

The possibility of seeing globular clusters (GC) in formation at high redshift and their possible role in cosmic reionization has been occasionally discussed in the literature, yet with rapidly growing interest as the operation of new major facilities (notably JWST and ELT) is approaching (see [Carlberg 2002](#); [Ricotti 2002](#); [Schraerer & Charbonnel 2011](#); [Katz & Ricotti 2013, 2014](#); [Trenti \*et al.\* 2015](#); [Renzini 2017](#); [Zick \*et al.\* 2018](#); [Boylan-Kolchin 2018](#)). First observational hints at objects that may be them can be found in [Vanzella \*et al.\* \(2016, 2017a,b, 2019\)](#), [Elmegreen \(2017\)](#) and [Bouwens \*et al.\* \(2017, 2018\)](#).

Figure 1 shows what is perhaps the best example of a just formed GC at  $z = 6.145$  from [Vanzella \*et al.\* \(2019\)](#). What we see is a galaxy highly magnified and stretched by cluster gravitational lensing, with object D1(core) appearing perfectly round in spite of the stretching, which sets an upper limit of only 13 pc to its half-light radius. Vanzella *et al.* estimate for it a mass of  $\sim 7 \times 10^5 M_\odot$  and an age of 10 Myr, thus redshift, size, mass and age appear to be what indeed we would expect a just formed GC should look like.

Most Milky Way GCs formed  $\sim 12.5 \pm 1$  Gyr ago (e.g., [Leaman, Vandenberg & Mendel 2013](#)), hence corresponding to redshifts beyond 3, when only  $\sim 6\%$  of the present day stellar mass was already formed ([Madau & Dickinson 2014](#)), which means that the bulk GC formation precedes the build up of massive galaxies, hence the observation of forming GCs can provide crucial information on the very early stages of galaxy formation.

In this contributed paper I build on the results of a recent attempt to calculate the expected number counts of GC progenitors (i.e., young GC at  $z > 3$ ), specifically for the early observations with JWST ([Pozzetti, Maraston & Renzini 2019](#)), then mentioning some of the opportunities offered by a follow-up with the ELT and its early instrumentation.

## 2. Number Counts

The number counts of any kind of astronomical precursor at high redshift is given by the sampled comoving volume times the local number density of the specific kind of astronomical objects. Examples are given in Table 1, where for a standard cosmology ( $\Omega_\Lambda = 0.7$ ,  $\Omega_M = 0.3$  and  $H_0 = 70$ ) the comoving volume between  $z = 3$  and 10 sampled by the  $\sim 10$  arcmin $^2$  field of view of the NIRCam camera on board JWST will be

**Table 1.** What to find at  $z > 3$  in a NIRCam frame ( $\sim 10$  arcmin $^2$ )

Object	Local Number Density [Mpc $^{-3}$ ]	Number of Precursors in a Frame
Galaxy Clusters & BCGs	$10^{-5}$	$\sim 1$
$M_* > 10^{11} M_\odot$ Galaxies	$2 \times 10^{-3}$	$\sim 200$
Globular Clusters	1.5	$\sim 200,000$
GCPs within 10 Myr	from peak luminosity	$\sim 1,500$

Note: The number of precursors within one NIRCam frame is given by the sampled comoving volume between  $z = 3$  and 10 ( $\sim 130,000$  Mpc $^3$ ) times the local number density of their progeny.

### Dense star forming complexes /clusters at $z = 6.145$

(Vanzella+17,19)

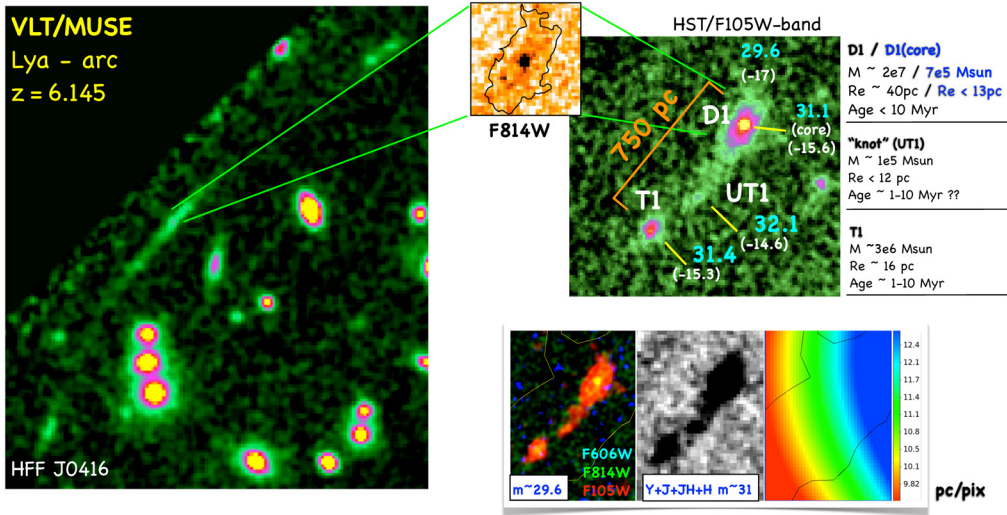


**Figure 1.** Zoomed-in images of a highly magnified and stretched galaxy at  $z = 6.145$  with its point-like core, less than 13 pc in size, offering a very plausible example of a just formed globular cluster. (Courtesy of Eros Vanzella).

$\sim 130,000$  Mpc $^3$ . Thus, given the local number density of GCs ( $\sim 1.5$  Mpc $^{-3}$ ) each NIRCam 10 arcmin $^2$  frame will include the precursors of some 200,000 GCs. Of course, the vast majority of them will be too faint for being detected, either because they had not yet started to form stars, or because the young GC progenitors (GCP) may have already faded below detectability. We estimate that only  $\sim 1,500$  among them will be caught within 10 Myr from their peak luminosity.

In this approach, in Pozzetti *et al.* we have calculated the expected number counts of GCPs starting from the following assumptions:

- The MW is not atypical, so most GCs in the Universe formed within the first  $\sim 2$  Gyr from the Big Bang, i.e., at  $z \gtrsim 3$ .
- The mass function of forming GCs in the early Universe is either 1) identical to the local GC mass function, i.e., a Gaussian with  $\log M_* = 5.3$  and  $\sigma = 0.52$  dex (Harris *et al.* 2014), or 2) a scaled-up version of it with  $\log M_* = 6.3$  (i.e.,  $10\times$  the local  $M_*$ ). The first option assumes that the stellar mass of GCs is constant in time (no mass loss of any kind), the second option assumes that GCs were 10 times more massive at formation. With this *mass budget factor* (MBF) varying from 1 to 10 we hope to bracket reality.
- GCPs are approximated as unreddened simple stellar populations (SSP) ignoring the possible contribution of emission lines to broad-band photometry.

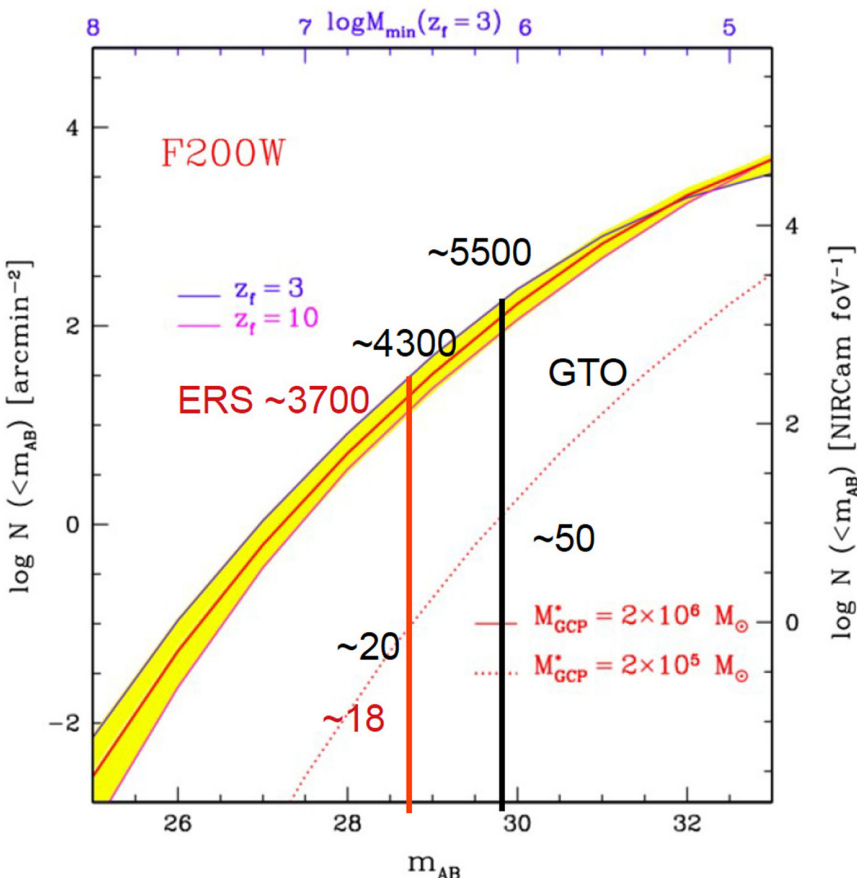


**Figure 2.** The expected number counts of globular cluster progenitors for the F200W filter of the NIRCam camera on JWST as from Pozzetti, Maraston & Renzini (2019). The upper scale gives the minimum mass a GCP should have in order to reach at its maximum luminosity the magnitude given in the lower scale. The dotted line correspond to assume a mass budget factor  $MBF=1$ , whereas the yellow band corresponds to  $MBF=10$ . The lower (magenta) bound of the yellow band refers to all GCPs forming at  $z=10$  whereas the upper (blue) bound refers to all forming at  $z=3$ . The red line in the middle refers to the case in which GCPs forms at constant rate in time, between  $z=10$  and  $z=3$ . The vertical lines show the limiting magnitudes that will be reached by the ERS and GTO observations with the NIRCam camera, with the corresponding numbers of GCP detections, respectively in red and black for ERS and GTO.

In Pozzetti *et al.* we extensively discuss justifications and limits for this set of assumptions, for example ignoring reddening may be reasonable for the metal poor half of the GCP population, but will certainly fail for the metal rich GCPs. In any event, we have calculated the expected number counts for all seven broad band filters of NIRCam, and under the two assumptions for the mass budget factor. As an example, Figure 2 shows the counts for the  $2\mu\text{m}$  (F200W) passband.

In this figure, the magenta line bordering the yellow band corresponds to all GCs forming at  $z=10$  and the blue line to all of them forming at  $z=3$ . The red line in the middle of the band corresponds to GCs forming at constant rate (in time, not redshift) between  $z=10$  and  $3$ . Clearly the expected number counts are fairly insensitive to the specific distribution of formation times provided they are restricted to the first few Gyr of cosmic time. As extensively illustrated in our paper, this insensitivity to formation

redshift is a direct consequence of the steep, near power-law shape of the rest-frame UV spectrum of young SSPs, with  $F(\lambda) \propto \lambda^{-\beta}$  with  $\beta \sim 2.5 - 3$ , ensuring a strong negative K-correction effect, such that in all bands the peak luminosity of young GCP is fairly insensitive to formation redshift. Number counts are instead extremely sensitive to the adopted mass budget factor, with Figure 2 showing that the predicted counts drop by over two orders of magnitude for the MBF changing from 10 to 1. Actual counts will therefore set interesting constraints on the initial mass of GCs.

The first opportunity for astronomers to check these numbers will be offered by the JWST/NIRCam “Early release Science” (ERS) observations which will cover  $\sim 100$  arcmin $^2$  down to mag  $\sim 29$ . As illustrated in Figure 2,  $\sim 3,700$  GCPs should be detected for MBF=10. This number falls down to  $\sim 18$  if MDF=1.

The next major deep sky coverage with NIRCam will be part of the guaranteed time observations (GTO), with the instrument team planning to reach mag  $\sim 29.8$  (at  $10\sigma$  for point sources) over 46 arcmin $^2$  and mag  $\sim 28.8$  over additional 190 arcmin $^2$ . Thus, all together ERS+GTO observations should detect (e.g., in F200W) from a minimum of  $\sim 90$  up to  $\sim 13,500$  GCPs for a MBF between 1 and 10, as indicated in Figure 2. These figures should be cut by a factor of  $\sim 2$  if the no reddening assumption is valid only for the metal poor GCPs.

### 3. Future ELT Follow-up of NIRCam Candidate GCPs

Among all these NIRCam candidates, how will we distinguish true GCPs from dwarfs galaxies or clusters of GCPs? At these redshifts, the spatial resolution of NIRCAM is  $\sim 200$  pc, largely insufficient to make such distinction. Lensing already can! as demonstrated by [Vanzella et al. \(2019\)](#) and [Bouwens et al. \(2018\)](#), but lensing will not provide the required mass production of GCPs, anytime soon.

The best opportunity will instead be offered by MICADO, the first-light instrument at the ELT ([Davies et al. 2016](#)). Assisted by multi-conjugate adaptive optics (MCAO), MICADO will be diffraction limited, and thanks to a telescope aperture of 39m will reach a resolution of  $\sim 30$  pc. MICADO should then do a great job in following-up NIRCam candidates, separating massive and compact objects, qualifying as GCPs, from more fluffy dwarfs that may host them, such as the complex object shown in Figure 1.

MICADO has a field of view  $53'' \times 53''$  ( $\sim 0.8$  arcmin $^2$ ) and on average should include  $\sim 80$  mag  $< 29.8$  GCPs for MBF=10, or just  $\sim 1$  for MBF=1. But ERS+GTO observations will also give  $\sim 30$   $z > 3$  progenitors to massive clusters of galaxies, with their M87-like BCG progenitors, each with its swarm of  $\sim 10,000$  GCPs. From Table 1 we expect, on average, one such system per NIRCam frame, so we will have a non negligible chance that one out of the 30 BCG progenitors will be caught near its firework peak of GC formation. With MICADO imaging all of them with  $\sim 30$  pc resolution!

MICADO will also be equipped with a narrow slit (16 mas, or  $\sim 80$  pc) spectrograph, allowing us to get redshifts of candidate GCPs from lines such as [OII] (up to  $z \sim 4.4$ ), CIV (up to  $z \sim 12$ ) and Ly $\alpha$  (for  $z > 5.5$ ).

The other ELT first-light instrument is HARMONI ([Thatte et al. 2016](#)), the diffraction limited ( $\sim 30$  pc resolution) integral field spectrograph, which will allow the spectroscopic separation of GCPs from their dwarf hosts. Like MICADO, also HARMONI will be especially fast on point-like sources, as GCPs would be.

Next instrument on the line (and relevant in this context) will be MOSAIC [Hammer et al. 2016](#), the multi-object spectrograph for the ELT. With its  $0''.1$  arcsec spaxels ( $\sim 500$  pc), a multiplex of  $\sim 100$  and a patrol field of  $\sim 40$  arcmin $^2$ , it will contain  $\sim 4,000$  dwarf galaxies at  $3 < z < 10$  brighter than mag  $\sim 28$ , and some 40 GCPs to the same limiting magnitude (for MBF=10).

With these perspectives ahead, how can we avoid being impatient?

## References

- Bouwens, R. J., Illingworth, G. D., Oesch, P. A., Atek, H., Lam, D., & Stefanon, M. 2017, *ApJ*, 843, 41  
Bouwens, R. J., Illingworth, G. D., Oesch, P. A., Labb  , I. *et al.* 2018, arXiv:1711.02090  
Boylan-Kolchin, M. 2018, *MNRAS*, 479, 332  
Carlberg, R. G. 2002, *ApJ*, 573, 60  
Davies, R. *et al.* 2016, SPIE.9908E.1Z  
Elmegreen, B. G. 2017, *ApJ*, 836, 80  
Hammer, F. *et al.* 2016, SPIE.9908E.24  
Harris, W. E. *et al.* 2014, *ApJ*, 797, 128  
Katz, H. & Ricotti, M. 2013, *MNRAS*, 432, 3250  
Katz, H. & Ricotti, M. 2014, *MNRAS*, 444, 2377  
Leaman, R., VandenBerg, D. A., & Mendel, J. T. 2013, *MNRAS*, 436, 122  
Madau, P. & Dickinson, M. 2014, *ARA&A*, 52, 415  
Pozzetti, L., Maraston, C., & Renzini, A. 2019, *MNRAS*, 485, 5861  
Ricotti, M. 2002, *MNRAS*, 336, L33  
Renzini, A. 2017, *MNRAS*, 469, L63  
Schraerer, D. & Charbonnel, C. 2011, *MNRAS*, 413, 2297  
Thatte, N. A. *et al.* 2016, SPIE.9908E.1X  
Trenti, M., Padoan, P., & Jimenez, R. 2015, *ApJ*, 808, L35  
Vanzella, E. *et al.* 2016, *ApJ*, 821, L27  
Vanzella, E. *et al.* 2017a, *MNRAS*, 467, 4304  
Vanzella, E. *et al.* 2017b, *MNRAS*, 465, 3803  
Vanzella, E. *et al.* 2019, *MNRAS*, 483, 3618  
Zick, T. O., Weisz, D. R., & Boylan-Kolchin, M. 2018, *MNRAS*, 477, 480